

Department of Pharmaceutics,  
Bombay college of Pharmacy,  
Santacruz (E), Mumbai-400 098,  
India

Rajendrakumar Kale, Pralhad  
Tayade

Department of Pharmacology,  
Bombay college of Pharmacy,  
Santacruz (E), Mumbai-400 098,  
India

Madhusudan Saraf

Anti-cancer Drug Screening  
Facility, Advanced Centre for  
Treatment, Research and  
Education in Cancer, Navi  
Mumbai 410 208, India

Aarti Juvekar

Y. T. Institute of Pharmacy,  
Karjat, Raigad-410 201, India

Pralhad Tayade

**Correspondence:** P. Tayade,  
Dept of Pharmaceutics, Bombay  
College of Pharmacy, Kalina,  
Santacruz (E), Mumbai-400 098,  
India. E-mail: pralhadtayade@  
yahoo.com

#### Acknowledgements and

**funding:** This work was funded  
by University Grants Commission  
(UGC) Govt. of India, New Delhi,  
India Major Research Grant F.3-  
64/2002 (SR-II), which is  
gratefully acknowledged. Special  
thanks to members of Anti-  
cancer Drug Screening Facility,  
Tata Memorial Centre, Advanced  
Centre for Training, Research  
and Education in Cancer  
(ACTREC), Navi Mumbai, India,  
for help in carrying out in-vitro  
anti-cancer drug screening  
experiments. One of the authors,  
Rajendrakumar Kale wishes to  
express deep sense of gratitude  
towards Mr Sanket Jadhav  
(Bombay College of Pharmacy)  
and Mr Madan Barkume  
(ACTREC) for the expertise  
provided during in-vivo animal  
experiments. The authors are  
grateful to Dr D. V. Behere,  
Department of Chemical  
Sciences, Tata Institute of  
Fundamental Research (TIFR)  
Mumbai, India, for providing the  
facility to perform CD  
spectroscopy experiments.

## Decreased B16F10 melanoma growth and impaired tumour vascularization in BDF1 mice with quercetin–cyclodextrin binary system

Rajendrakumar Kale, Madhusudan Saraf, Aarti Juvekar and Pralhad Tayade

### Abstract

The aim of this work was to study the inclusion behaviour of a poorly water-soluble bioflavonoid, quercetin, towards sulfobutyl ether-7 $\beta$ -cyclodextrin. It also involves angiogenesis inhibition in-vivo in addition to in-vitro human cancer cell growth inhibition study of quercetin and its cyclodextrin complex. Drug–cyclodextrin solid inclusion complexes were prepared and characterized in solution and in the solid state. An in-vitro anti-proliferation study using plain drug and its solubilized form was carried out on human cancer cell lines of different origin. Further, an in-vivo tumour growth inhibition study was carried out using a mouse melanoma model. Histological sections of tumours were examined for the evaluation of tumour microvessel density. Significant enhancement of the solubility and dissolution rate of the quercetin, which occurred after complexation, might be attributed to the decrease in crystallinity of drug. SBE7 $\beta$ CD complex of quercetin was more potent for inhibiting cell proliferation in human erythroleukaemia and cervix cancer cells. Decreased tumour microvessel density in mouse melanoma after oral quercetin administration led to diminished tumour cell proliferation. Quercetin–SBE7 $\beta$ CD complex showed significantly improved anti-cancer activity at much lower concentration than the plain drug, providing evidence for dose reduction without affecting therapeutic efficacy when using cyclodextrin carriers.

### Introduction

Flavonoids have a broad pharmacological profile, such as anti-lipoperoxidant, anti-inflammatory properties and the ability to exert anti-cancer and chemopreventive effects (Verma et al 1988; Cassady 1990; Bosisio & Pirola 1992; Abad et al 1993). Animal studies and investigations using different cellular models suggested that certain flavonoids could inhibit tumour initiation as well as tumour progression, and major molecular mechanisms of action include anti-proliferation, cell-cycle arrest, induction of apoptosis and inhibition of the angiogenic process (Ren et al 2003). There are few contrary reports that may be due to differences in bioavailability (due to poor aqueous solubility) of the various flavonoids, and their effects on individual cancer sites cannot be excluded, meriting further investigation (Garcia et al 1999).

Quercetin, 3,3',4',5',7'-pentahydroxy flavone, a polyphenolic flavonoid, extremely hydrophobic in nature, is a component of onion. Quercetin has several biological effects, including a strong inhibitory effect on the growth of several human and animal cancer cell lines, and enhances the anti-proliferative effect of cisplatin both in-vitro and in-vivo (Larocca et al 1990; Scambia et al 1990). Despite this wide spectrum of pharmacological properties, its use in the pharmaceutical field is limited by its low aqueous solubility. In recent years, cyclodextrin complexation has been successfully used to improve solubility, chemical stability and bioavailability of a number of poorly soluble compounds. Recently, various hydrophilic, hydrophobic and ionic cyclodextrin derivatives have been successfully utilized to extend the physicochemical properties and inclusion capacity of natural cyclodextrin (Hirayama & Uekama 1999; Ono et al 2001). All the data obtained from FT-IR, DSC, X-ray diffraction and SEM studies for the study of freeze-dried quercetin–cyclodextrin binary systems using  $\beta$ -cyclodextrin ( $\beta$ CD) and hydroxypropyl- $\beta$ -cyclodextrin (HP $\beta$ CD) have shown that it is possible to obtain an inclusion complex with a stoichiometry of 1:1, in the

solid-state and in aqueous solution, with an overall complexing ability that is slightly greater for the HP $\beta$ CD derivative (Tayade & Kale 2004).

In this study, solubilization of quercetin was achieved by complexation with the sulfobutyl ether-7 derivative of  $\beta$  cyclodextrin (SBE7 $\beta$ CD).  $^1\text{H}$  NMR and circular dichroism (CD) spectroscopy study was carried out to confirm the host-guest interactions in the solution state. Additional information on the complexing efficacy of the cyclodextrin toward quercetin in the solid state was obtained by differential scanning calorimetry (DSC), Fourier transform infrared (FTIR) spectroscopy (FT-IR) and X-ray powder diffractometry (XRD) studies. We have also evaluated the effect of the SBE7 $\beta$ CD complex of quercetin on the proliferation of various human cancer cell lines in-vitro, in comparison with free drug. In-vivo tumour growth inhibitory activity and tumour angiogenesis inhibition after oral administration of quercetin and its SBE7 $\beta$ CD complex was also studied using B16F10 mouse melanoma model.

## Materials and Methods

### Materials

Quercetin was purchased from S.D. Fine Chemicals (Mumbai). Sulfobutyl ether-7 $\beta$ -cyclodextrin (SBE7 $\beta$ CD; Captisol<sup>®</sup>; average degree of substitution, 6.5) was kindly provided by Cydex Inc. (Overland Park). Human cancer cell cultures were obtained from the National Cancer Institute (USA). RPMI-1640 medium and fetal bovine serum (FBS) were purchased from Gibco Corp. (NJ). Sulforhodamine B (SRB) dye was bought from Sigma Chemical Co. All sterile plastic-wares were procured from Nunc Inc. (Denmark). All other reagents and solvents used were procured locally and were of analytical grade.

### Phase solubility study

The method of Higuchi & Connors (1965) was followed. An excess amount of drug was added to 10 mL of water or an aqueous solution of cyclodextrin (0.0025–0.0125 M concentration range) in 25-mL stoppered conical flasks and shaken at  $27 \pm 1.0^\circ\text{C}$ . At equilibrium after 24 h, samples were withdrawn, filtered (0.45  $\mu\text{m}$  pore size) and spectrophotometrically assayed for drug content at 372 nm. Each experiment was carried out in triplicate (coefficient of variation (CV) < 3%). The apparent binding constant of the quercetin-cyclodextrin complex was calculated from the slope and intercept of the straight line of the phase-solubility diagram.

### Circular dichroism spectroscopy

Circular dichroism spectra were obtained by a Jasco J-600 Spectropolarimeter. Absorbances of the samples were kept below 2 in the whole wavelength range explored (200–300 nm). All the spectra were corrected for the signal exhibited by the SBE7 $\beta$ CD solution in the absence of the guest. The signal-to-noise ratio was improved by superposition of five different scans.

### Nuclear magnetic resonance (NMR) spectroscopy

$^1\text{H}$  NMR spectra were recorded using a Bruker AVANCE 500 DRX (500 MHz) instrument. The samples for NMR measurement were prepared in 0.6 mL of  $\text{CD}_3\text{OD}:\text{D}_2\text{O}$  (1:1 v/v) mixture.

### Preparation of solid inclusion complexes

#### *Kneading with aqueous ethanol (KN)*

Kneaded product was prepared in a 1:1 molar ratio by wetting drug-cyclodextrin physical mixture in a mortar with the minimum volume of ethanol-water (1:1 v/v) mixture and kneading thoroughly with a pestle to obtain a paste, which was then dried under vacuum at room temperature and stored in a desiccator until further evaluation.

#### *Co-evaporation from aqueous ethanol (COE)*

Co-evaporated product was prepared by co-evaporation of equimolar drug-CD ethanol-water (1:1 v/v) solutions on a water bath at  $60^\circ\text{C}$ .

Each solid product was passed through an 80-mesh sieve and the same fraction was used for the following tests. Physical mixture (PM) was obtained by tumble mixing equimolar amounts of 80-mesh fractions of respective simple components for 10 min.

### Physico-chemical characterization of inclusion complexes

#### *Differential scanning calorimetry (DSC)*

A Shimadzu-Thermal Analyzer DT 40 was used for recording DSC thermograms of the quercetin raw material, inclusion complexes as well as the physical mixture. Samples (2–8 mg) were heated in an open aluminium pan at a rate of  $10^\circ\text{C min}^{-1}$  between 30 and  $330^\circ\text{C}$  temperature range under a nitrogen flow of  $40 \text{ mL min}^{-1}$ .

#### *Fourier transform infrared (FTIR) spectroscopy*

Fourier transform IR spectra were recorded on a Jasco FTIR-5300 spectrophotometer. The spectra were recorded for quercetin, its cyclodextrin complexes and physical mixture. Samples were prepared in KBr disks. The scanning range was  $450\text{--}4000 \text{ cm}^{-1}$  and the resolution was  $4 \text{ cm}^{-1}$ .

#### *X-ray powder diffractometry (XRD)*

X-ray powder diffractograms of quercetin raw material, inclusion complexes as well as the physical mixture were recorded on a Jeol JDX 8030 powder X-ray diffractometer using Ni-filtered,  $\text{CuK}\alpha$  radiation, a voltage of 40 kV and a 25 mA current. The scanning rate employed was  $1^\circ \text{ min}^{-1}$  over the  $10\text{--}40^\circ 2\theta$  (diffraction angle) range.

### In-vitro dissolution rate study

Dissolution rate experiments were performed in pH 7.4 phosphate buffer with 0.8% sodium lauryl sulfate (SLS) at  $37 \pm 0.5^\circ\text{C}$ , using USP XXI/XXII apparatus with the paddle stirrer rotating at  $50 \text{ rev min}^{-1}$ . At fixed time intervals, samples

were withdrawn, filtered and assayed spectrophotometrically for drug content at 372 nm.

### In-vitro cell proliferation assay

Human cancer cell lines were cultured in RPMI-1640 medium supplemented with FBS (10%) at 37°C and maintained in a CO<sub>2</sub> incubator in an atmosphere of 5% CO<sub>2</sub> in Nunc Tissue culture flasks. Cultures (70% confluent) were used to determine the cytotoxic effects of the quercetin and its cyclodextrin complex. The cells were seeded in 96-well microtitre-plates (at a concentration of  $1 \times 10^4$  cells/well) and incubated for 24 h to ensure adequate growth before determination of cell growth inhibition. After 24 h from seeding, test compounds were added in triplicate in different lanes of the wells, keeping the first lane as untreated control and the last lane for adriamycin, a positive control.

Cytotoxicity caused by the test compounds was evaluated using the SRB assay protocol (Skehan et al 1990). Briefly, the cells were further incubated at 37°C in a CO<sub>2</sub> incubator for 48 h. These non-adherent cell cultures were then fixed in-situ by slow addition of cold 50% trichloroacetic acid (TCA). The plate was then kept at 4°C for 60 min. The supernatant was discarded and all the wells were washed 5 times with water. Plates were then air-dried. SRB solution (0.4% w/v in 1% acetic acid) was added to each of the wells and the plate was kept at room temperature for 20 min. The unbound dye was removed by washing 5 times with 1% acetic acid. The plate was flicked several times to remove traces of moisture, followed by air-drying. Bound dye was then extracted by addition of 10 mM Tris base (pH 10.5) to each of the wells. Optical density was measured at 540 nm on an ELISA microplate reader. Cell number was derived from a calibration curve set up with known number of cells.

### Tumour growth inhibitory activity using B16F10 mouse melanoma model

Female BDF1 mice each were subcutaneously inoculated in the abdominal region with  $10^6$  B16F10 cells in sterile PBS, and this day was considered day zero. The untreated control group was given orally 0.2 mL of 0.25% carboxymethylcellulose (CMC) in PBS, while the test groups were administered orally with plain quercetin ( $50 \text{ mg kg}^{-1}$  and  $25 \text{ mg kg}^{-1}$ ) or SBE7 $\beta$ CD complex (equivalent to  $50 \text{ mg kg}^{-1}$  and  $25 \text{ mg kg}^{-1}$  of quercetin), or both, suspended/dissolved in PBS containing 0.25% CMC, beginning on day 1 every 48 h for a total of 10 doses.

Tumour diameters were measured every other day with a slide calliper and tumour volume calculated using the formula:  $\text{volume (mm}^3\text{)} = \text{width}^2 \text{ (mm}^2\text{)} \times \text{length (mm)} \times 0.52$ . Three weeks after inoculation, mice were sacrificed by cervical dislocation and tumours were excised and stored in 10% phosphate-buffered formalin until further evaluation.

### Tumour microvessel density evaluation

For tumour microvessel localization, the tumours were processed using an auto-technicon apparatus through increasing concentrations of ethanol and infiltrated in paraffin (melting

point 58–60°C). To evaluate microvessel density within the tumour mass, histological sections of 5  $\mu\text{m}$  thick were obtained. Sections were stained with haematoxylin–eosin. The slides were observed independently under low-power microscopy and the angiogenesis response (tumour microvessel density) was recorded as 4 (marked), 3 (moderate), 2 (mild), 1 (minimal) and 0 (negative).

### Statistical methods

The results of in-vitro dissolution rate study are expressed as mean  $\pm$  standard deviation (s.d.) of three independent measurements. The results of in-vitro cell proliferation assay are expressed as mean  $\pm$  s.d. of three experiments with six replicates each. The tumour volume measurement results are expressed as mean  $\pm$  s.d. for four mice in each group. The effect of plain drug, its physical mixture and inclusion complexes with cyclodextrin was examined using Kruskal–Wallis test. Individual differences between various formulations were then examined using Tukey's HSD test. The effect of concentration and type of formulation on % cell growth inhibition was studied by two-way analysis of variance. The effect of formulation type and time on tumour volume of mice was compared using a repeated measures analysis of variance. Individual differences between different formulation types at respective dose level were studied using a Dunnett's post-hoc test. The effect of formulation type on degree of angiogenesis was examined using Kruskal–Wallis test followed by Tukey's HSD and Dunnett's post-hoc tests for determining differences between individual treatments.

## Results and Discussion

### Phase solubility study

A linear relationship between the amount of quercetin solubilized and the concentration of cyclodextrin in solution was observed (Figure 1). According to Higuchi & Connors (1965), this may be attributed to the formation of soluble 1:1 molar ratio inclusion complex with the stability constant of  $423 \text{ M}^{-1}$ .

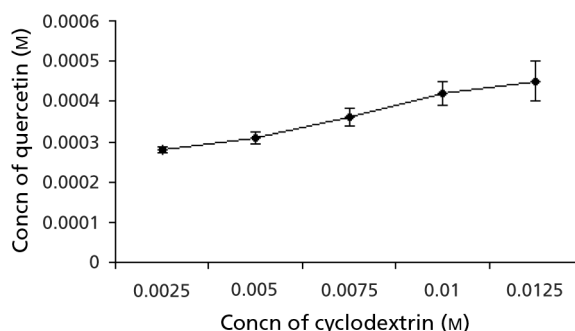


**Figure 1** Phase solubility diagram of quercetin–SBE7 $\beta$ CD system. Each data point and error bars represent a mean  $\pm$  s.d. of three determinations.

### Circular dichroism spectroscopy

Quercetin shows a characteristic UV absorption spectrum due to the presence of chromophores but alone it gave no circular dichroism band at experimental conditions studied, because it has no asymmetric carbon atom in the molecule. When SBE7 $\beta$ CD was added to the quercetin solution, a Cotton effect was observed in the wavelength range of 200–270 nm. In the presence of SBE7 $\beta$ CD, quercetin showed a strong positive peak at 230 nm and relatively small negative peaks at 210 nm and 255 nm as a result of perturbation of the electronic transition of the drug caused by the asymmetric cavity of cyclodextrin following complexation. The spectral modifications observed in the presence of SBE7 $\beta$ CD can be considered the effect of a stronger interaction of SBE7 $\beta$ CD with quercetin in confirmation of phase solubility study and high polarizability of O–S bond in SBE7 $\beta$ CD (Ikeda et al 1975).

It is well known that cyclodextrins have neither circular dichroism nor absorption band at wavelengths longer than 220 nm and the inclusion of optically inactive compounds within the cyclodextrin cavity generates extrinsic Cotton effect in the wavelength region of drug chromophores. Thus, the circular dichroism spectroscopic data indicate that quercetin is embedded in the asymmetric locus of the SBE7 $\beta$ CD cavity.

### NMR spectroscopy

One-dimensional proton NMR spectra were recorded for the plain quercetin sample and quercetin with SBE7 $\beta$ CD. Chemically, quercetin is composed of two aromatic cycles, benzopyran-4-one and 3, 4 dihydroxy-phenyl ring. When the one dimensional NMR spectrum of quercetin was compared with that of quercetin–SBE7 $\beta$ CD spectrum, it was seen that there were obvious chemical shift differences for the aromatic protons of quercetin. A significant downfield shift for the resonance of aromatic protons, H<sub>c</sub> and H<sub>b</sub> of the benzopyrone ring of quercetin was observed in the presence of Captisol (Figure 2). Similarly, the signals of aromatic protons H<sub>d</sub>, H<sub>e</sub> and H<sub>f</sub> of the dihydroxyphenyl ring of quercetin showed differences in chemical shift (downfield shift) but were comparable with that of plain drug.

The significant downfield shift noted for the resonance of the aromatic protons of benzopyrone ring of quercetin in the <sup>1</sup>H NMR spectra of quercetin–SBE7 $\beta$ CD binary system suggest that the drug molecule interacts with the cyclodextrin cavity, providing an inclusion complex. Moreover, the result of NMR study was in accordance with initial inspection of the structure of quercetin, suggesting that the benzopyrone ring moiety would be expected to be included within the cavity of Captisol due to its higher hydrophobicity in comparison with the dihydroxy phenyl ring of quercetin.

### Physical characterization

#### DSC

Quercetin is a dihydrate molecule and in the DSC thermogram it showed a broad endothermic peak ( $T_{\text{peak}} = 101^{\circ}\text{C}$ ) as it becomes anhydrous and a melting endotherm ( $T_{\text{onset}} = 322.8^{\circ}\text{C}$ ;  $T_{\text{peak}} = 326.2^{\circ}\text{C}$ ) (Figure 3). SBE7 $\beta$ CD is

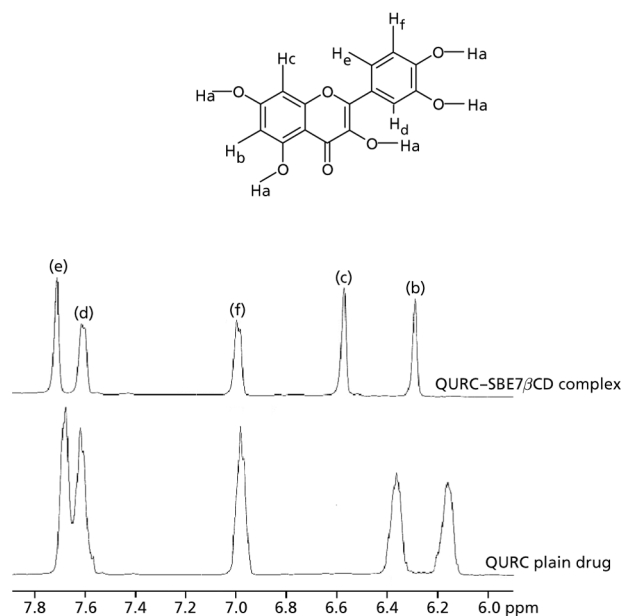


**Figure 2** <sup>1</sup>H NMR spectra of free quercetin (QURC) and QURC–SBE7 $\beta$ CD complex.

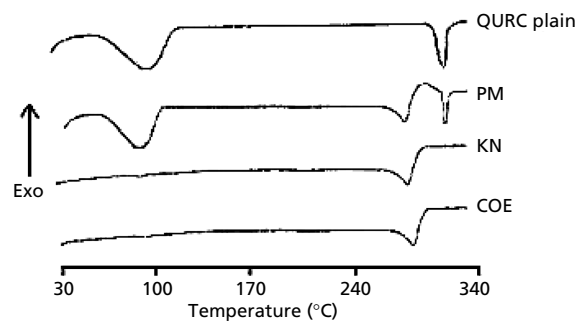


**Figure 3** DSC thermograms of plain quercetin (QURC) and its binary systems with SBE7 $\beta$ CD. PM, physical mixture; KN, kneading with aqueous ethanol; COE, co-evaporation from aqueous ethanol.

an amorphous material and shows a broad endotherm over approximately 40–150°C consistent with dehydration of the sample. Decomposition event begins at approximately 260°C. The characteristic, well recognizable, thermal profile of the drug appeared at the temperature corresponding to its melting point in the physical mixture of drug with cyclodextrin. Complete disappearance of the drug endothermic peak for drug–cyclodextrin systems obtained by kneading and co-evaporation was observed. This phenomenon can be assumed as proof of interactions between the components of the respective binary systems and can be considered indicative of drug amorphization or inclusion complex formation (Kim et al 1985).

#### FTIR spectroscopy

Drug crystals show a characteristic carbonyl absorption band at  $1664.72\text{ cm}^{-1}$ , assigned to aromatic ketonic carbonyl

stretching in the FTIR spectra. The FTIR spectra of the drug-CD complex were compared with those of the physical mixture and pure drug. In the case of kneaded and co-evaporated products, in particular, the characteristic aromatic carbonyl-stretching band of drug appeared shifted to  $1653.14\text{ cm}^{-1}$  with reduced intensity and broadening of the band. Changes in the characteristic band of pure drug in the FTIR spectra confirm the existence of the inclusion complex as a new compound with different spectroscopic bands (Ficarra et al 2002).

### XRD

In the X-ray diffractogram of quercetin powder, sharp peaks at a diffraction angle ( $2\theta$ ) of  $12.48^\circ$ ,  $15.86^\circ$ ,  $23.88^\circ$  and  $24.88^\circ$  were present, suggesting that the drug is present as a crystalline material. Drug crystallinity peaks were detectable in the physical mixture with SBE7 $\beta$ CD wherein the X-ray diffraction pattern of the inclusion complex of quercetin was devoid of any sharp drug crystallinity peaks and characterized only by large diffraction peaks. It means a total drug amorphization was induced by complexation where it was no longer possible to distinguish the characteristic crystallinity peaks of flavonoid in the X-ray diffractogram of quercetin-SBE7 $\beta$ CD solid complex. These results confirm that quercetin is no longer present as a crystalline material and its solid inclusion complex exists in the amorphous state with SBE7 $\beta$ CD.

### In-vitro dissolution

The results in terms of dissolution efficiency and percent of active ingredient dissolved at 5 min are collected in Table 1. It is evident that the binary systems with cyclodextrin exhibited faster dissolution rates than plain quercetin as 50% drug dissolved in first 5 min. The dissolution efficiencies of co-evaporated and kneaded products were 1.4–1.5 times higher than that of the corresponding physical mixture and 1.8 to 1.9 times higher than that of plain drug, respectively. A statistically significant difference was found for DP<sub>5</sub> (% drug dissolved at 5 min) and DE<sub>60</sub> (dissolution efficiency over a period of 60 min) between plain drug, its physical mixture and cyclodextrin complexes (Kruskal–Wallis test,  $P < 0.05$ ) whereas the individ-

**Table 1** Dissolution parameters of quercetin (QURC) alone and its equimolar physical mixture (PM), kneaded (KN) and co-evaporated (COE) product with SBE7 $\beta$ CD

Sample		DP <sub>5</sub>	DE <sub>60</sub>
QURC plain		$29.5 \pm 2.84^a$	$34.4 \pm 3.17^{a'}$
QURC-SBE7 $\beta$ CD	PM	$32.0 \pm 1.75^{ab}$	$43.6 \pm 2.40^{a'b'}$
	KN	$49.5 \pm 0.75^{abc}$	$65.6 \pm 0.64^{a'b'c'}$
	COE	$47.4 \pm 1.25^{abc}$	$63.4 \pm 1.75^{a'b'c'}$

Values are expressed as mean  $\pm$  s.d. for 3 measurements. Comparisons are made between: <sup>a,a'</sup>QURC plain, PM, KN and COE (statistically significant, Kruskal–Wallis test,  $P < 0.05$ ); <sup>b,b'</sup>PM, KN and COE (statistically significant, Tukey's HSD test,  $\alpha = 0.05$ ); <sup>c,c'</sup>KN and COE (statistically insignificant, Tukey's HSD test,  $\alpha = 0.05$ ).

ual difference between plain drug and its physical mixture with SBE7 $\beta$ CD was statistically insignificant (Tukey's HSD test,  $\alpha = 0.05$ ). Concerning the significant enhancement of the dissolution rate that occurred with binary products, this might be attributed to an increase of solubility upon complexation, due to the amorphization generally occurring during complexation (i.e. a decrease in crystallinity).

### In-vitro cell proliferation

Both quercetin and its SBE7 $\beta$ CD complex showed very good anti-proliferative activity (>50% cell growth inhibition) towards all human cancer cells tested, in-vitro. The activity of plain quercetin was concentration dependent, maximum activity being obtained at the highest concentration tested ( $80\text{ }\mu\text{g mL}^{-1}$ ). However, in the case of SiHa cervix cancer cells and K562 human erythroleukaemia cells, the anti-proliferative effect of quercetin-SBE7 $\beta$ CD complex was found to be improved but statistically not significant (two way analysis of variance,  $P > 0.05$ ) as compared with that of plain quercetin (Figure 4).

Quercetin-SBE7 $\beta$ CD complex showed more than 50% inhibition of cell growth at a concentration of  $10\text{ }\mu\text{g mL}^{-1}$  (i.e. 8 times improvement in the activity of plain drug when it has been included in the cavity of cyclodextrin). The improved anti-proliferative activity of quercetin in the presence of cyclodextrin can be considered the effect of improved cell permeation of the drug as cyclodextrin keeps the drug molecules in solution and delivers them to the surface of the cell membrane where they partition into, and through, the membrane whenever equilibrium is disturbed (Loftsson et al 1994).

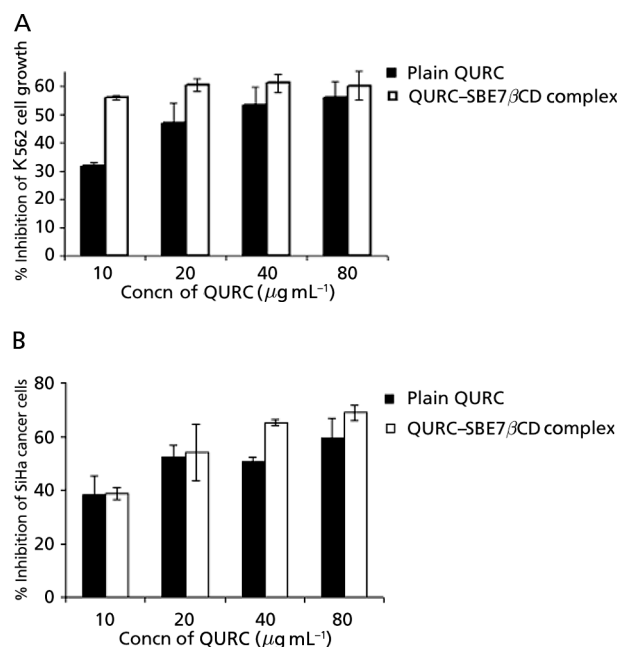


**Figure 4** In-vitro % cell growth inhibition for K562 human erythroleukaemia cells (A) and SiHa cervix cancer cells (B) using quercetin (QURC) and its SBE7 $\beta$ CD complex. Each data point and error bars represent a mean  $\pm$  s.d. of three experiments with six replicates each.

### Tumour growth inhibition

To examine whether the notable increase in anti-proliferative activity in-vitro observed with cyclodextrin–quercetin binary system may lead to differences in pharmacological effects in-vivo, we explored the tumour growth inhibition profiles of quercetin and quercetin–SBE7 $\beta$ CD complex using a mouse melanoma model. The Institutional Ethics Committee for Animal Care and Use of Advanced Centre for Treatment, Research and Education, Navi Mumbai, India has approved the animal study protocol. The Oral Solution Formulation Protocol for the use of SBE7 $\beta$ CD in experimental animals was also approved by Cydex Inc., USA.

From Table 2, it is evident that B16F10 melanoma cells injected subcutaneously into mice grew to an average size of 1800 mm<sup>3</sup>. Treatment of mice with plain quercetin resulted in significant inhibition of tumour growth as compared with control. Quercetin at a dose of 25 and 50 mg kg<sup>-1</sup> body weight showed about 90 and 93% inhibition of mouse melanoma growth, respectively. Thus when drugs were given at specified doses through both forms, each tumour volume of the plain-drug-treated group and the drug–cyclodextrin-treated group was considerably reduced; the % tumour growth inhibition was significantly improved for the product with cyclodextrin (repeated measures analysis of variance,  $P < 0.05$ ). In addition, as in the case of in-vitro cell growth inhibition experiments, oral administration of SBE7 $\beta$ CD–quercetin complex exhibited improved anti-cancer activity in terms of tumour growth delay in mice in contrast to animals in control and plain-drug treatment groups. But the observed significant

**Table 2** Mean tumour volume (mm<sup>3</sup>) at 9, 11, 13, 15, 17, 19 and 21 days since tumour cell inoculation after oral administration of plain quercetin and its SBE7 $\beta$ CD complex to mice

<b>I</b> Days	<b>Control*</b>	<b>Plain drug (50 mg kg<sup>-1</sup>)*</b>	<b>SBE7<math>\beta</math>CD complex (equivalent to 50 mg kg<sup>-1</sup> drug)*</b>
9	2.64 $\pm$ 1.55	NTD	NTD
11	3.88 $\pm$ 2.09	0.78 $\pm$ 0.38	0.52 $\pm$ 0.30
13	24.10 $\pm$ 22.13	1.80 $\pm$ 1.27	2.69 $\pm$ 1.35
15	238.93 $\pm$ 14.49	6.99 $\pm$ 5.11	3.40 $\pm$ 2.36
17	827.56 $\pm$ 38.92	71.90 $\pm$ 19.25	6.91 $\pm$ 2.38
19	1369.1 $\pm$ 82.27	94.34 $\pm$ 15.92	7.80 $\pm$ 1.87
21	1755.84 $\pm$ 98.03	115.98 $\pm$ 11.59	8.68 $\pm$ 0.76
<b>II</b> Days	<b>Control*</b>	<b>Plain drug (25 mg kg<sup>-1</sup>)*</b>	<b>SBE7<math>\beta</math>CD complex (equivalent to 25 mg kg<sup>-1</sup> drug)*</b>
9	2.64 $\pm$ 1.55	NTD	NTD
11	3.88 $\pm$ 2.09	1.02 $\pm$ 0.52	1.05 $\pm$ 0.3
13	24.10 $\pm$ 22.13	3.20 $\pm$ 1.35	1.65 $\pm$ 1.88
15	238.93 $\pm$ 14.49	37.84 $\pm$ 5.12	8.62 $\pm$ 5.15
17	827.56 $\pm$ 38.92	109.09 $\pm$ 14.66	41.47 $\pm$ 4.60
19	1369.10 $\pm$ 82.27	125.40 $\pm$ 13.92	49.19 $\pm$ 3.94
21	1755.84 $\pm$ 98.03	173.97 $\pm$ 17.65	82.98 $\pm$ 7.69

The tumour volume measurements are expressed as mean  $\pm$  s.d. for 4 mice in each group. \* $P < 0.05$  (repeated measures analysis of variance). NTD, no tumour detected.

difference for tumour regression between plain drug and its cyclodextrin complexes was not constant over time (treatment days). This non-significant result (repeated measures analysis of variance,  $P > 0.05$ ) suggests that the pattern of response to treatment is similar for the two formulations. A reasonable conclusion based on this analysis is that the cyclodextrin complex is effective (superior to plain drug alone) and that its advantage beyond the plain drug is approximately maintained during the course of the experiment.

These results could be attributed to higher drug availability at the tumour site due to the faster and complete drug absorption in the presence of cyclodextrin. Consequently, cyclodextrin potentially serves as a drug reservoir, replenishing the free drug concentration at the membrane surface by rapid dissociation as equilibrium is disturbed following drug absorption. The driving concentration for drug absorption can thus be maintained, as the formulation/drug is retained at the membrane surface in its solubilized state in the presence of cyclodextrin.

### Tumour microvessel density evaluation

Accumulating evidence demonstrates that tumour growth and lethality are dependent on angiogenesis. Therefore to investigate whether decreased tumour growth by quercetin in mice was attributable to decreased host angiogenesis, we evaluated the microvessel density in tumour sections. Representative photographs of melanoma tumours after excision and photomicrographs of stained tumour microsections (Figure 5) showed that a marked/dense microvasculature was observed in the control tumours. The tumour angiogenesis response (tumour microvessel density median value) recorded for control tumours, plain drug and cyclodextrin-complex-treated tumour was 3, 1.5 and 1, respectively. Tumours treated with plain drug had significantly fewer microvessels (Dunnett's test,  $\alpha = 0.05$ ) compared with the control. In fact, as evident from Figure 5, the anti-angiogenesis effect was significantly improved in the tumours of mice receiving drug–cyclodextrin complex in comparison with plain drug and control group (Tukey's HSD test and Dunnett's test,  $\alpha = 0.05$ ).

The findings of tumour microvessel density evaluation suggest that quercetin suppressed the expression of angiogenic vascularization in melanoma tumours. It is well known that inflammatory mediators contribute to the process of angiogenesis and some of the inflammatory prostaglandins, products of arachidonic acid metabolism, are pro-angiogenic (Jackson et al 1997). Quercetin also exerts anti-inflammatory activity through its antioxidant and inhibitory effects on inflammation-producing enzymes (cyclooxygenase, lipoxigenase) and the subsequent inhibition of inflammatory mediators, including leukotrienes and prostaglandins (Della et al 1988). It is to be noted that the in-vivo processes, including hypoxia, growth factor production, cytokine-activated COX-2 induction, prostaglandin production, VEGF-mediated vascular permeability and neovascularization, are strikingly similar. As quercetin has inhibitory activity against inflammation-producing enzymes and other inflammatory mediators, the anti-angiogenic activity of quercetin could be ascribed to the inhibition of cyclooxygenase enzyme or leukotrienes and prostaglandin production.

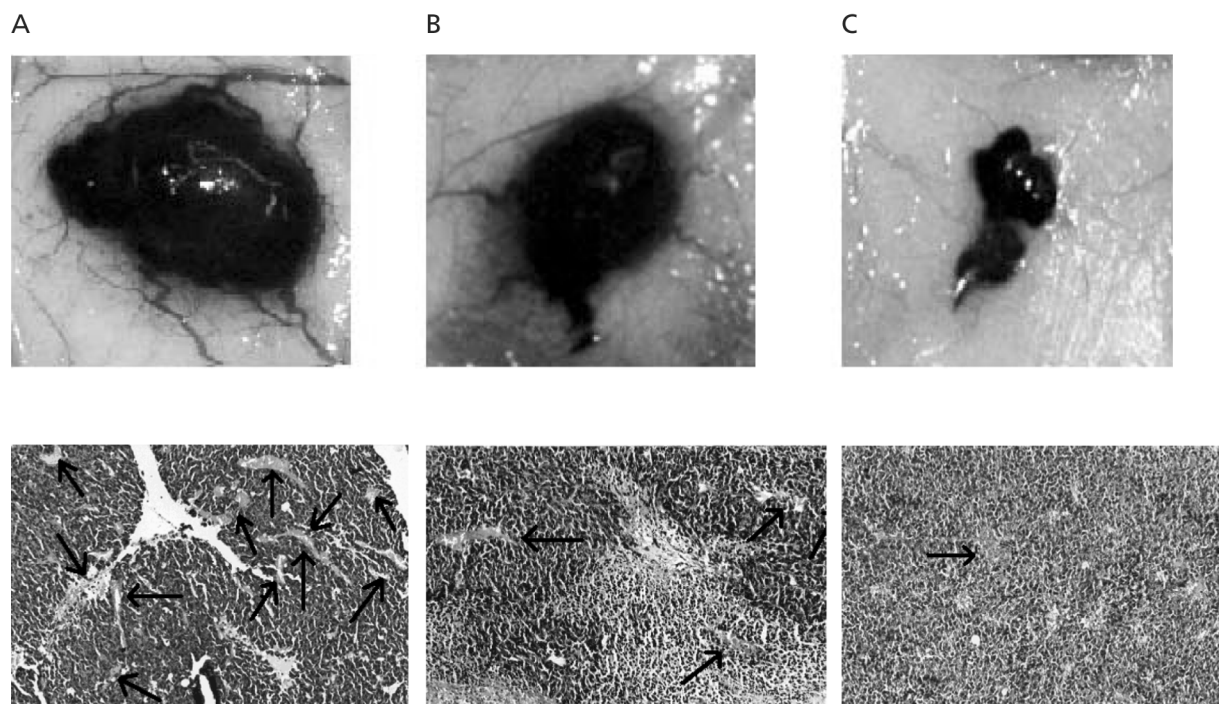


**Figure 5** Tumour sprouting vasculature after tumour excision and presence of microvasculature (indicated by arrows) in tumour microsections after staining. In control tumours (A), dense microvasculature appeared throughout the tumour section whereas tumour microvessel density was significantly reduced in plain-drug-treated ( $50 \text{ mg kg}^{-1}$ ) mouse tumours (B) and cyclodextrin-complex (equivalent to  $50 \text{ mg kg}^{-1}$  plain drug)-treated mice (C).

The improved angiogenesis inhibition observed with drug–cyclodextrin combination treatment may be attributed to the high drug accumulation inside the tumour. It can be considered the effect of high drug availability at the absorption site, attributable to solubilization by cyclodextrins and improved cell permeation of the drug molecule as a consequence of membrane lipid extraction caused by the cyclodextrin (Boulmedarat et al 2004).

## Conclusions

Through complexation with SBE7 $\beta$ CD, the aqueous solubility of quercetin has been improved substantially in neutral aqueous solutions. Thus, SBE7 $\beta$ CD is useful in improving the dissolution and the bioavailability of quercetin in pharmaceutical formulation. Quercetin–SBE7 $\beta$ CD complex showed significantly improved in-vivo anti-cancer property compared with the plain drug, providing evidence for dose reduction without affecting therapeutic efficacy when using cyclodextrin carriers.

## References

- Abad, M., Bermejo, P., Villar, A., Vaverdes, S. (1993) Anti-inflammatory activity of two flavonoids from *Tanacetum microphyllum*. *J. Nat. Prod.* **56**: 1164–1167
- Bosisio, B., Pirola, O. (1992) Effect of the flavanolignans of *Silybum marianum* L. on lipid peroxidation in rat liver microsomes and freshly isolated hepatocytes. *Pharmacol. Res.* **25**: 147–154
- Boulmedarat, L., Bochot, A., Lesieur, S., Fattal, E. (2004) Toward the mechanism of destabilization of lipid membranes by methylated beta cyclodextrins. Presented at *12th International Cyclodextrin Symposium*, Montpellier, France. Abstract book, p. 8.
- Cassady, J. (1990) Natural products as a source of potential cancer chemotherapeutic and chemopreventive agents. *J. Nat. Prod.* **53**: 23–41
- Della, L., Ragazzi, E., Tubaro, A. (1988) Anti-inflammatory activity of benzopyrones that are inhibitors of cyclo- and lipo-oxygenase. *Pharmacol. Res. Commun.* **20**: S91–S94
- Ficarra, R., Tommasini, S., Raneri, D., Calabro, M., Di Bella, M., Rustichelli, C., Gamberini, M., Ficarra, P. (2002) *J. Pharm. Biomed. Anal.* **29**: 1005–1014
- Garcia, R., Gonzalez, A., Agudo, A., Riboli, E. (1999) High intake of specific carotenoids and flavonoids does not reduce the risk of bladder cancer. *Nutr. Cancer* **35**: 212–214
- Higuchi, T., Connors, K. A. (1965) Phase solubility techniques. *Adv. Anal. Chem. Inst.* **4**: 117–212
- Hirayama, F., Uekama, K. (1999) Cyclodextrin based controlled drug release system. *Adv. Drug Deliv. Rev.* **36**: 125–141
- Ikeda, K., Uekama, K., Otagiri, M. (1975) Inclusion complexes of  $\beta$ -cyclodextrin with anti-inflammatory drug fenamates in aqueous solution. *Chem. Pharm. Bull.* **23**: 201–208
- Jackson, J., Seed, M., Kircher, C., Willoughby D., Winkler, J. (1997) The codependence of angiogenesis and chronic inflammation. *FASEB J.* **11**: 457–465
- Kim, K., Frank M., Henderson, N. (1985) Applications of differential scanning calorimetry to the study of solid drug dispersions. *J. Pharm. Sci.* **74**: 283–289
- Larocca, L., Piantelli, M., Leone, G. (1990) Type II oestrogen binding sites in acute lymphoid and myeloid leukaemias: growth inhibitory effect of oestrogen and flavonoids. *Br. J. Haematol.* **75**: 489–495

- Loftsson, T., Friourisdottir, H., Ingvarsdottir, G., Jonsdottir B., Siguroardottir, A. (1994) The influence of 2-hydroxypropyl-cyclodextrin on diffusion rates and transdermal delivery of hydrocortisone. *Drug Dev. Ind. Pharm.* **20**: 1699–1708
- Ono, N., Arima, H., Hirayama, F., Uekama, K. (2001) A moderate interaction of maltosyl- $\alpha$ -cyclodextrin with Caco-2 cells in comparison with the parent cyclodextrin. *Biol. Pharm. Bull.* **24**: 395–402
- Ren, W., Qiao, Z., Wang, H., Zhu, L., Zhang, L. (2003) Flavonoids: promising anticancer agents. *Med. Res. Rev.* **23**: 519–534
- Scambia, G., Ranelletti, F., Panici, P. (1990) Inhibitory effect of quercetin on OVCA 433 cells and presence of type II oestrogen binding sites in primary ovarian tumours and cultured cells. *Br. J. Cancer* **62**: 942–946
- Skehan, P., Strong, R., Scudiero, D., Monks, A., McMahon, J., Vistica, D. (1990) New colorimetric cytotoxicity assay for anticancer drug screening. *J. Natl Cancer Inst.* **83**: 1107–1112
- Tayade, P., Kale, R. (2004) Study of freeze-dried quercetin-cyclodextrin binary systems by DSC, FT-IR, X-ray diffraction and SEM analysis. *J. Pharm. Biomed. Anal.* **34**: 333–339
- Verma, A., Johnson, J., Gould, M., Tanner, M. (1988) Inhibition of 7,12-dimethylbenz (a) anthracene- and N-nitrosomethylurea-induced rat mammary cancer by dietary flavonol quercetin. *Cancer Res.* **48**: 5754–5758